An aerodynamic bearing with adjustable geometry and self-lifting capacity Part 1: self-lift capacity by squeeze film

D N Ha[1], **T A Stolarski**[1]*, and **S Yoshimoto**[2]
[1]Brunel University, Uxbridge, Middlesex, UK
[2]Tokyo University of Science, Tokyo, Japan

The MS was received on 24 March 2004 and was accepted after revision for publication on 4 October 2004.

DOI: 10.1243/135065005X9682

Abstract: An aerodynamic bearing capable of self-lift by squeeze film is presented. The bearing uses piezoelectric actuators and elastic hinges in order elastically to deform the initial cylindrical clearance to a three-lobe clearance. The three-lobe clearance can cyclically deform with sufficient amplitude and frequency to generate a squeeze-film pressure. This squeeze-film separates the shaft and bearing surfaces, and eliminates rubbing of the two surfaces at low rotational speeds. Numerical and experimental results show that, although the proposed bearing has a relatively low squeeze-film load capacity, it is practically feasible.

Keywords: journal bearing, squeeze-film bearing, elastic hinges

1 INTRODUCTION

The increasing demand for high-speed and high-precision applications gives rise to the need for air-lubricated bearings. Owing to the compressibility of air, when operated at sufficiently high rotational speeds, plain cylindrical aerodynamic bearings suffer from dynamic instabilities, such as the 'half-frequency whirl'. An attempt to run the bearing above twice its critical speed can lead to spiral growth of the orbit and eventually to a direct contact between the shaft and bearings. The stability of cylindrical aerodynamic bearings can be improved by changing their geometry. However, a non-circular geometry, incorporating recesses, holes, steps, grooves, etc., not only increases the cost of manufacturing but also affects the pressure distribution in the lubricating film. Recently, a three-wave bearing was introduced [**1**]. This bearing has a sinusoidally varying bearing clearance. Numerical and experimental results show that the bearing is characterized by an impressive stability and good load capacity.

Corresponding author: Department of Mechanical Engineering, Brunel University, Uxbridge, Middlesex UB8 3PH, UK.

Although aerodynamic bearings are capable of self-generating pressure at high rotational speeds, they do suffer much wear and power loss during the start-up stages and shutdown. This is why hybrid bearings are the only solution in most practical applications. In hybrid bearings, the self-acting mechanism is supplemented with an external pressure source. However, the use of external compressors and tubing to supply the aerostatic pressure proves to be troublesome.

The squeeze-film action is another mechanism that could be used to generate pressure. Squeeze-film bearings, in the form of floating pads and linear sliders, proved to be effective for non-contacting systems [**2**–**5**]. However, most squeeze-film bearing designs are restricted by the size and specification of the driving piezoelectric actuators. Use of elastic hinges for squeeze-film bearings gave much flexibility in their design and proved to be very successful for miniaturization [**2**].

The aerodynamic bearing presented in this paper has the unique feature of a controllable geometry owing to the use of elastic hinges. The bearing also has the capability of generating squeeze-film pressure for the initial lift during the start-up stage. This paper introduces the bearing and presents

experimental and numerical results pertinent to its operation.

2 BEARING DESIGN AND OPERATION

Figure 1 shows a configuration of the bearing with six piezoelectric actuators (stack type) mounted in the slots machined in the bearing shell (two in each slot). In response to an applied voltage, the piezoelectric actuators expand and exert a force onto the bearing. Owing to the purposeful arrangement of the elastic hinges, the bearing shell deforms elastically from a perfect circle to a three-lobe geometry, as shown in Fig. 2. Adjusting the offset voltages applied to the piezoelectric actuators can accurately control the size of the deformation. The housing does not deform and prevents any deformation of the bearing shell on its outer periphery.

Owing to the properties of the piezoelectric actuators, an oscillating applied voltage will result in an oscillating motion, where the actuators expand and contract at the frequency of the oscillating voltage. By cyclically changing the circular bore to the dynamic three-lobe bore at an appropriate amplitude and frequency, a squeeze-film pressure is generated between the shaft and the bearing. This squeeze-film pressure allows the shaft to lift off from the bearing surface during start-up. Next, the rotation of the shaft is introduced, and, when the speed of the shaft reaches a magnitude securing

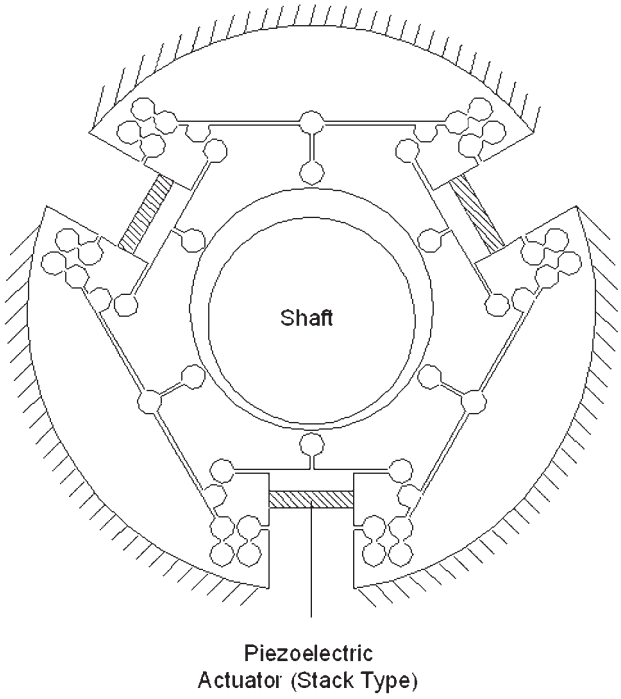

Fig. 1 Bearing with piezoelectric actuators and shaft (not to scale)

Fig. 2 Elastic deformation of the bearing by the piezoelectric actuators, creating a three-lobe bearing clearance

aerodynamic lift, the cyclic deformations of the bearing are terminated. The static (offset) deformation is retained in order to maintain the three-lobe bore configuration. Furthermore, while the shaft is rotating, the size of the static three-lobe bore can be adjusted according to the dynamic stability requirements.

A test bearing was fabricated for investigation. The bearing is made of stainless steel with a nominal bore diameter of 30.12 mm and a length of 25 mm. Piezoelectric actuators were used with a maximum displacement of 8 μm at an input voltage of 150 V. By assuming linear elastic deformation, finite element analysis predicts an unsymmetrical three-lobe bearing clearance. With 60 V input, the amplitudes of the three-lobe bore are 1.9133 and 1.6303 μm respectively. Measurements with a non-contacting eddy current probe showed lower values. This discrepancy is due to the curvature of the measured bearing surface and was corrected accordingly. Figure 3 shows good agreement between the experimental and finite element results. The three-lobe clearance profile is determined by the actuator input voltage and forms the film thickness equations.

3 NUMERICAL ANALYSIS FOR SQUEEZE-FILM PRESSURE

Figure 4 shows a schematic configuration view of the bearing and shaft. By assuming no eccentricity in the horizontal direction but only in the vertical direction, and by considering the film thickness as being thin

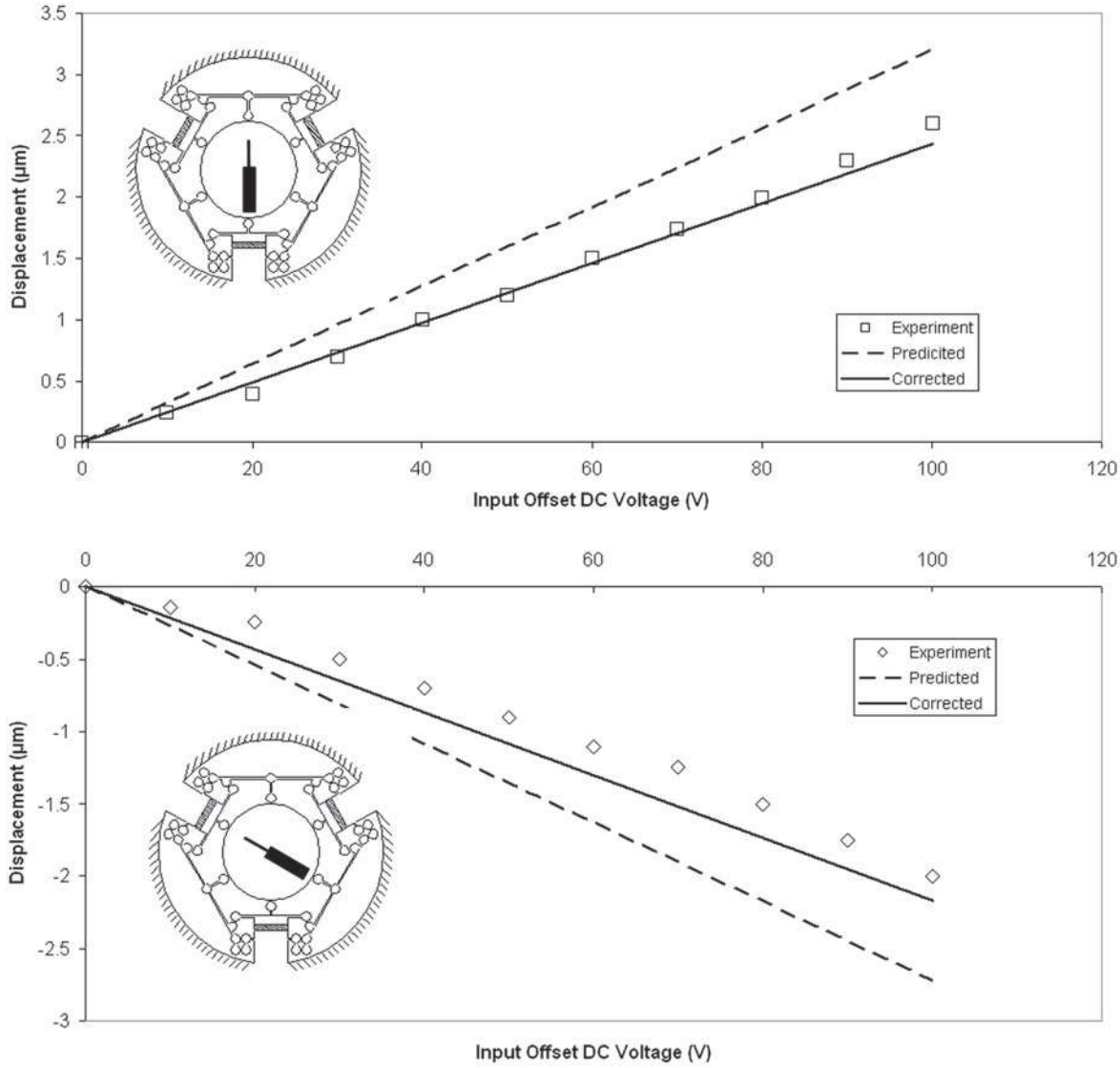

Fig. 3 Amplitudes of the three lobes of the bearing with input voltage

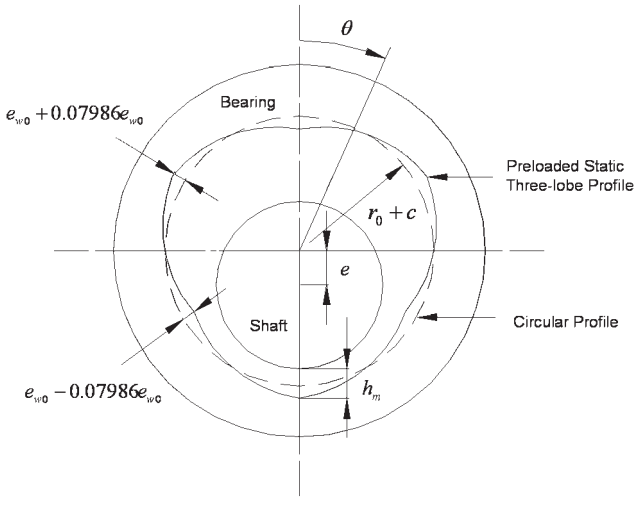

Fig. 4 Static three-lobe geometry of the bearing (not to scale)

when compared with other bearing dimensions, the air film between the non-rotating shaft and the bearing can be analysed as an unwrapped 2π film. The static three-lobe fluid film profile can be described as

$$h_{w0} = c + e\cos\theta - e_{w0}\cos(3\theta) + |0.07986e_{w0}\cos(3\theta)| \quad (1)$$

However, for squeeze-film lift, an oscillating standing wave is imposed, with oscillating amplitude e_w, where $e_w \leqslant e_{w0}$. This dynamic standing wave motion can be represented as

$$h_w = -e_w\sin(\overline{\omega}t)\cos(3\theta) + |0.07986e_w\sin(\overline{\omega}t)\cos(3\theta)| \quad (2)$$

Therefore, the total time dependent film thickness

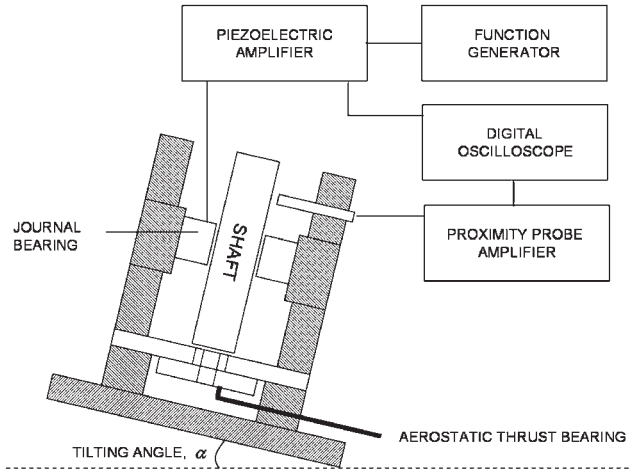

Fig. 5 Schematic of the experimental apparatus

can be represented as

$$h = h_{w0} + h_w \tag{3}$$

For the bottom film thickness when $\theta = \pi$

$$\begin{aligned} h|_{\theta=\pi} &= h_m \\ h_m &= c - e + 1.07986e_{w0} + 1.07986e_w \sin(\omega t) \\ \dot{h}_m &= \dot{e} + 1.07986\overline{\omega}e_w \cos(\omega t) \\ \ddot{h}_m &= \ddot{e} - 1.07986\overline{\omega}^2 e_w \sin(\omega t) \end{aligned} \tag{4}$$

The equation of motion for the shaft is

$$m_0\ddot{h}_m = f_p - m_\alpha g$$

where f_p is the pressure force and can be obtained by integration of the pressure as

$$f_p = -\int_0^{l_0}\int_0^{2\pi r_0} p\cos(x)\,\mathrm{d}x\,\mathrm{d}z \tag{5}$$

$$m_0\ddot{e} = 1.07986m_0\overline{\omega}^2 e_w \sin(\omega t) + f_p - m_\alpha g \tag{6}$$

Normalizing equation (6) with the following dimensionless quantities

$$\varepsilon = \frac{e}{c}, \qquad \varepsilon_w = \frac{e_w}{c}, \qquad \tau = \overline{\omega}t, \qquad P = \frac{p}{p_0},$$

$$\theta = \frac{x}{r_0}, \qquad Z = \frac{z}{r_0}$$

yields

$$\ddot{\varepsilon} = 1.1415\varepsilon_w \sin(\tau) + \frac{p_0 r_0^2}{m_0 c\overline{\omega}^2}F_p - \frac{m_\alpha g}{m_0 c\overline{\omega}^2} \tag{7}$$

where, $F_p = -\int\int P\cos(\underline{\theta})\,\mathrm{d}\theta\,\mathrm{d}Z$.

The pressure force, F_p, determines the lift capacity of the squeeze film. This pressure force is governed by the Reynolds equation in its non-dimensional form

$$\frac{\partial}{\partial\theta}\left(PH^3\frac{\partial P}{\partial\theta}\right) + \frac{\partial}{\partial Z}\left(PH^3\frac{\partial P}{\partial Z}\right) = \sigma\frac{\partial(PH)}{\partial\tau} \tag{8}$$

The squeeze number is defined as

$$\sigma = \frac{12\mu\overline{\omega}r_0^2}{p_0 c^2} \tag{9}$$

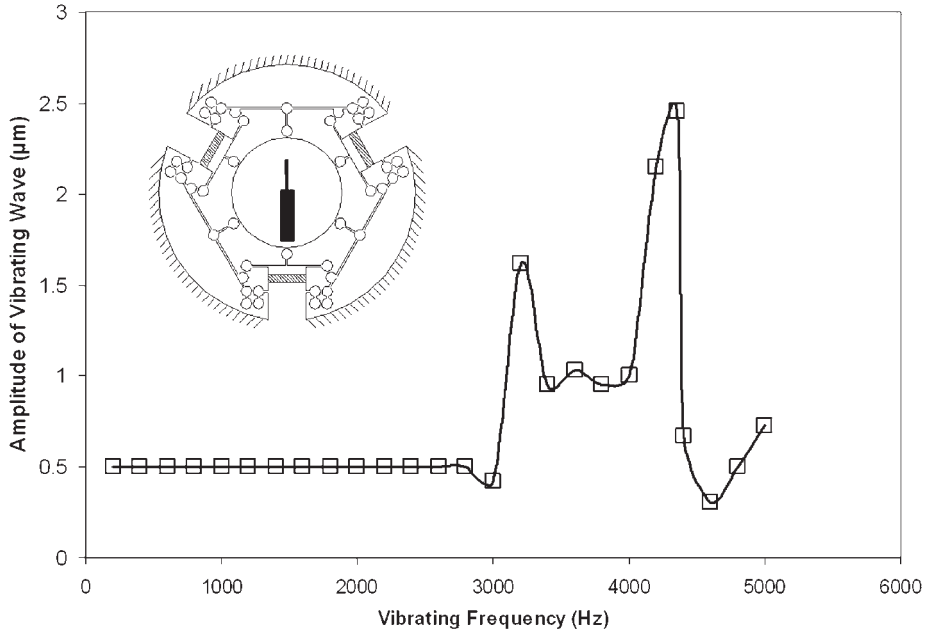

Fig. 6 Measured amplitudes of vibration at certain frequency

Table 1 Test parameters for the experiments

Variable	Settings	Values
m_α	5°, 10°, 15°, 20° tilt	56.65 g, 113.4 g, 170.2 g, 222.3 g
m_0	n/a	650 g
c	n/a	40 μm
e_{w0}	60 V	1.77 μm
e_w	30 V, 40 V, 50 V	0.45 μm, 0.65 μm, 0.85 μm
$\overline{\omega}/2\pi$	800–2800 Hz	800–2800 Hz

and

$$H = \frac{h}{c} = 1 + \varepsilon\cos\theta - \varepsilon_{w0}\cos(3\theta) + |0.07986\varepsilon_{w0}\cos(3\theta)| - \varepsilon_w\sin(\tau)\cos(3\theta) + |0.07986\varepsilon_w\sin(\overline{\omega}t)\cos(3\theta)| \quad (10)$$

The Reynolds equation was discretized using an implicit finite difference method (FDM) and solved iteratively using an underrelaxation technique. The pressure force, F_p, was then obtained by integrating the pressure over the spatial dimensions using Simpson's rule. The time dependent film thickness was obtained from the equation of motion [equation (7)] using Euler's method. However, the film thickness H (or the eccentricity ratio ε), being dependent on pressure P, results in the coupling of equations (7) and (8). Treatment of the coupled equations involves the iterative solutions of P and ε. Convergence is reached when ε converges to a steady state, i.e. when the pressure force balances the applied loading. Owing to periodicity, it is only necessary to evaluate one cycle.

With initial conditions, when $t = 0$

$$P = 1, \qquad \varepsilon = 0$$

With boundary conditions

$$P|_{Z=0} = 1, \qquad \left.\frac{\partial P}{\partial Z}\right|_{Z=1/2} = 0$$

For continuous film

$$P|_{\theta=0} = P|_{\theta=2\pi}$$

For constant periodicity

$$P|_\tau = P|_{\tau+2\pi}, \qquad H|_\tau = H|_{\tau+2\pi}$$

4 EXPERIMENTAL APPARATUS AND PROCEDURE

Figure 5 shows the arrangement of the experimental apparatus. A tilting test rig was built to determine the squeeze-film load capacity of the journal bearing. A stainless steel shaft of 30.04 mm diameter gave a circular bearing clearance of 40 μm. The aerostatic thrust ensures that the shaft floats freely during testing. A piezoelectric amplifier and a frequency

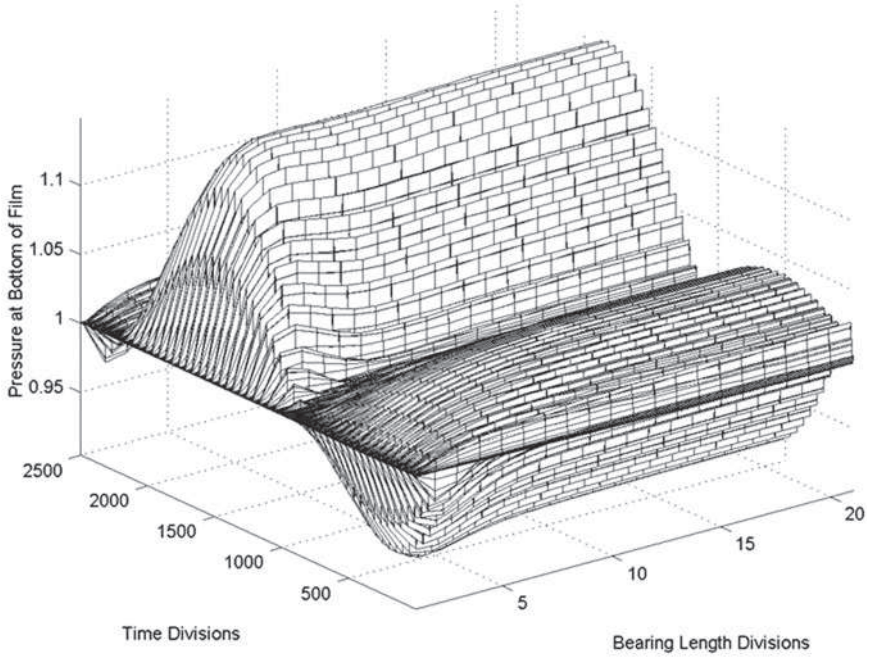

Fig. 7 Typical pressure profile of the fluid film for one cycle: $\varepsilon = 0.87$, $e_w = 0.65$ μm, $e_{w0} = 1.7718$ μm

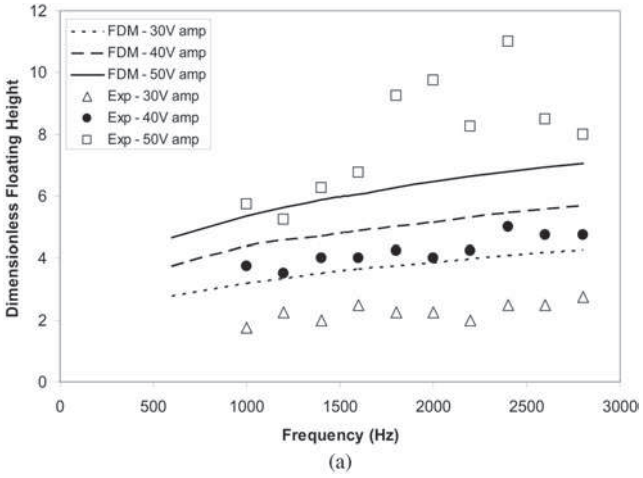

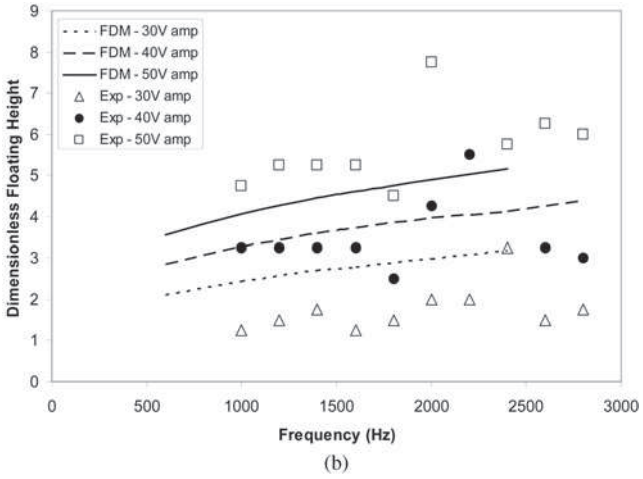

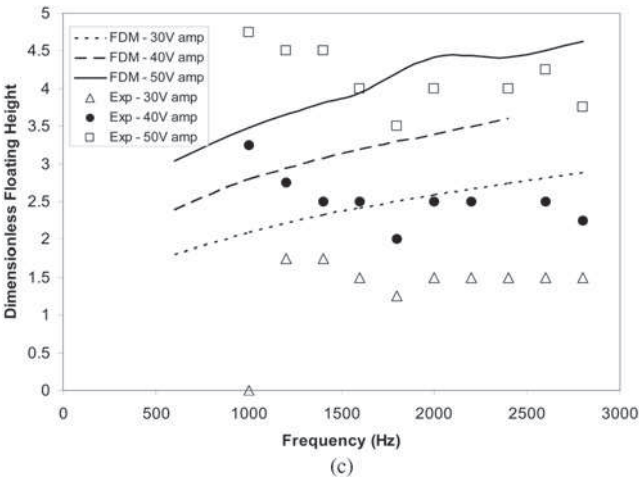

Fig. 8 Comparison between numerical and experimental results at steady state: (a) 56.65 g loading; (b) 113.4 g loading; (c) 170.2 g loading; (d) 222.3 g loading

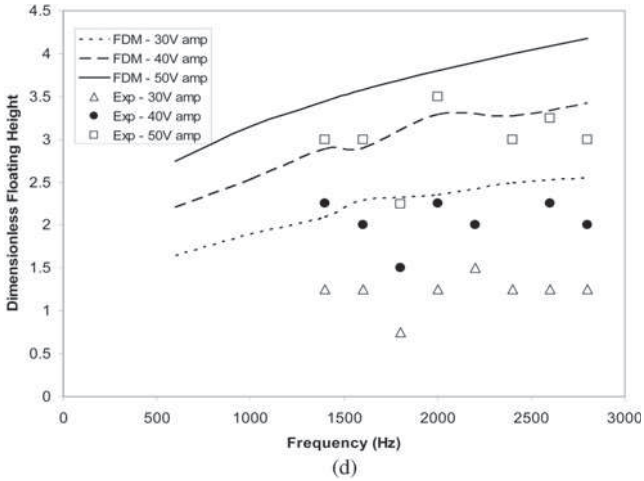

Fig. 8 Continued

generator control the operation of the journal bearing. This gave some control on the squeeze-film amplitudes and frequency. The shaft lift-off by squeeze-film pressure is measured using non-contact eddy current sensors. The housing is magnetically clamped onto a tilting chuck and, by tilting the housing, the loading imposed on the bearing by the shaft can be adjusted. Figure 6 shows remarkably large amplitudes of shaft vibration measured at 3.2 kHz and above. However, the measured values did not consider the effect of the fluid stiffness and damping effect on the bearing. Hence, the natural frequencies of the bearing are affected by the operating condition of the bearing.

Although some bearings are designed to operate at resonance frequencies [**4**, **5**], the present study investigated frequencies of up to 2.8 kHz, where the effect of resonance is negligible. The test parameters for the experiments are summarized in Table 1.

5 RESULTS AND DISCUSSIONS

It was found experimentally that the dynamic characteristics of the piezoelectric actuators differ from its static characteristics. An offset 60 V d.c. gave a larger stroke than that of an oscillating 60 V peak a.c.

The pressure profile in Fig. 7 shows a time-averaged pressure greater than ambient pressure, resulting from the compressibility of the fluid [**3**–**5**]. In the present work, the loading was kept constant for each set of tests, so the load capacity of the bearing could be measured by the floating height of the shaft. A larger separation between the bearing and shaft would clearly indicate a higher load capacity.

Figure 8a shows the relationships between the floating height of the shaft and the squeeze-film frequency. The experimental and numerical results show good qualitative agreement; the floating height increases with increasing vibrating amplitudes, exemplified by

a larger voltage. However, the effect of frequency on shaft levitation is rather unclear from the experimental results.

Figures 8a to d show that increasing the imposed load results in smaller floating heights. The bearing can support a static load of 2.18 N with a minimum film thickness of 1.5 μm. This suggests that the bearing has a rather low load capacity. The load capacity of the squeeze-film is mainly limited by the performance of the piezoelectric actuators. The bearing performance can be improved by utilizing piezoelectric actuators with larger stroke lengths to give larger amplitudes of vibration.

Below 800 Hz the tests show that there is insufficient squeeze-film pressure to support any load, and above 2800 Hz the bearing vibrated chaotically with very large amplitudes on account of resonance. Although shaft levitation was evident at the resonance modes, it was also observed that the shaft started to rotate at a speed and direction that changed with the modes of vibration. This phenomenon is believed to be the result of the unsymmetrical pressure distribution created by the bearing at the resonant conditions.

6 CONCLUDING REMARKS

In this paper, an aerodynamic journal bearing that uses hinges for elastic deformation of the bearing clearance geometry is presented. The bearing is designed to generate aerodynamic and squeeze-film pressures. The purpose of squeeze-film pressure was to initiate self-lift during the start-up stage. The numerical and experimental results show good agreement. With a vibrating amplitude and frequency of 0.45 μm and 1400 kHz respectively, sufficient squeeze-film pressure was generated by the bearing to support a load of up to 2.18 N.

REFERENCES

1 **Dimofte, F.** Wave journal bearing with compressible lubricant. Part 1: the wave bearing concept and a comparison to the plain circular bearing. *STLE Tribology Trans.*, 1995, **38**(1), 153–160.

2 **Yoshimoto, S., Anno, Y., Sato, Y.,** and **Hamanaka, K.** Float characteristics of squeeze-film gas bearing with elastic hinges for linear motion guide. *Jap. Soc. Mech. Engrs Int. J., Ser. C*, 1997, **40**(2), 353–359.

3 **Salbu, E. O. J.** Compressible squeeze films and squeeze bearings. *Trans. ASME, Ser. D, J. Basic Engng*, 1964, **86**, 355–364.

4 **Wiesendanger, M., Probst, U.,** and **Siegwart, R.** Squeeze film air bearings using piezoelectric bending elements. In proceedings of 5th International Conference on *Motion and Vibration Control (MOVIC 2000)*, Sydney, 2000, pp. 181–186.

5 **Minikes, A.** and **Bucher, I.** Coupled dynamics of a squeeze-film levitated mass and a vibrating piezoelectric disc: numerical analysis and experimental study. *J. Sound and Vibr.*, 2003, **263**, 241–268.

APPENDIX: Notation

c	undeformed radial bearing clearance
e	shaft vertical eccentricity
e_{w}	dynamic amplitude of the three-lobe motion
e_{w0}	static amplitude of the three-lobe bearing clearance
f_p	force due to pressure
F_p	dimensionless force due to pressure
g	acceleration due to gravity
h	film thickness
h_{m}	film thickness at the bottom when $\theta = \pi$
h_{w}	dynamic standing wave motion
h_{w0}	static three-lobe bearing clearance
l_0	bearing length
m_α	mass of the load
m_0	mass of the shaft
p	pressure
p_0	ambient pressure
P	dimensionless pressure $= p/p_0$
r_0	radius of the circular film
t	time
x	circumferential displacement
z	length displacement
Z	dimensionless bearing length displacement $= z/r_0$
α	tilting angle
ε	eccentricity ratio $= e/c$
ε_{w}	dimensionless dynamic amplitude of the three-lobe motion $= e_{\mathrm{w}}/c$
$\varepsilon_{\mathrm{w0}}$	dimensionless static amplitude $= e_{\mathrm{w0}}/c$
θ	angular length of the film
μ	viscosity of the fluid
σ	squeeze number $= (12\mu\overline{\omega}r_0^2)/(p_0c^2)$
τ	dimensionless time $= \overline{\omega}t$
$\overline{\omega}$	frequency of the three-lobe motion